Simulation Study of Integrated Solar Combined Cycle Systems: Medium Scale Plant in Irbid City

Khalideh Al bkoor Alrawashdeh[1*], Huthaifa Ahmad Al_issa[2], Ahmed A. Hussien[1], Isam Qasem[1], La'aly A. Al-Samrraie[3], Kamel K. Al-Zboon[3]

[1] Mechanical Engineering Department, Al-Huson University College, Al-Balqa' Applied University, P.O. Box 50, Al-Huson, Irbid 19117, Jordan

[2] Electrical Engineering Department, Al-Huson University College, Al-Balqa' Applied University, P.O. Box 50, Al-Huson, Irbid 19117, Jordan

[3] Water and Environmental Engineering Department, Al-Huson University College, Al-Balqa' Applied University, P.O. Box 50, Al-Huson, Irbid 19117, Jordan

Corresponding Author Email: khalideh19@bau.edu.jo

ABSTRACT

This study deals with an integrated solar combined cycle systems (ISCCS) simulation. The ISCCS presents a cogeneration of the Parabolic Trough Solar collector (PTC) system and the Rankine power cycle. The PTC system is employed to ensure stable thermal energy which is required to operate a steam turbine (with three stages), which is designed to produce enough electrical power (medium scale). The performance of the ISCCS is simulated and evaluated by using the TRNSYS software. This system is being considered for installation in Irbid, Jordan, and a comparison study is being conducted to determine the performance of the ISCCS – medium scale during the winter and summer seasons. The results show that the ISCRCS system's efficiency is 14.3% in winter (January 1) and 21.2% in summer (August 1), with 4.48 MW of electrical power produced in winter (January 1) and 4.05 MW produced in summer (August 1).

1. INTRODUCTION

Jordan suffers from a permanent energy crisis and imports 97% of its energy, which requires about 15% of its gross domestic product [1]. The complexity of the immediate changes in global fuel prices has increased as a result of this state. Jordan's energy problem needs solutions that are compatible with general available conditions. Jordan's weather and its location offer high solar energy that can be exploited in an integrated manner through modern techniques.

Concentrating Solar Power (CSP) and thermodynamics plants can be a great method and solution to the problem of energy production in many regions of the Middle East and, especially, in Jordan. Electric power demands a large quantity of energy to operate, and can theoretically be associated with the solar system [2]. There are several technologies depending on the temperature range; Flat plate and evacuated tube collectors provide from low temperature up to 100°C and compound parabolic collectors and parabolic trough from medium temperature up to 400°C [3, 4]. Various industrial processes require heat temperatures of from 100–650°C [5-9]. The fundamental challenges to achieving the execution of these technologies are the process type, the applications, the heat requirements, and the ranges of temperature [10, 11].

Modeling and simulation are essential tools for incorporating solar thermal systems (STS) into thermal processes because they allow for the prediction of system performance [12, 13]. Furthermore, administering different designs is needed to choose the most applicable one for each specific application, without the need to evaluate many available resources, both time and economically.

In the literature, models have been improved by tracking the performance of STS using various software and validating it with theoretical and experimental data [10-12]. Studies on the integration, potential, and control of solar thermal plants have been conducted [5-8, 14]. Several models have also been investigated by TRNSYS software (Transient System Simulation Tool), which is an analyzable modular simulation software that permits the thermodynamic simulation of energy techniques, and thus is principally used to simulate facilities containing systems that operate with the solar thermal system [13, 14]. The efficiency of the results obtained using the TRNSYS software predicts the performance of the STS adequately. Several studies have developed other simulation tools using programs in languages like JAVA and C++ [13]. The solar thermal systems' performance was investigated by developing modeling [15-17]. Integration, potential and monitoring of integrated thermal plants was carried out by using several programs and software [18-22].

The solar electric generation systems were the start of the integrated solar combined cycle systems ISCCS [23]. The ISCCS is considered being the largest plant with 75 MW of solar energy output and 354 MW of electrical power produced [24]. The characteristics of ISCCS with parabolic trough solar collector (PTC) were investigated and discussed [25].

Overall, the efficiency of the ISCCS type of PTC co-junction with Rankine cycle was evaluated as high efficiency, which can reach up to 32 percent [20] in comparison with the solar electric generation systems were the start of the integrated solar combined cycle systems ISCCS [23]. The

ISCCS is considered to be the largest plant, with 75 MW of solar energy output and 354 MW of electrical power produced [24]. The characteristics of ISCCS with a parabolic trough solar collector (PTC) were investigated and discussed [25].

Overall, the efficiency of the ISCCS type of PTC co-junction with the Rankine cycle was evaluated as high efficiency, which can reach up to 32 percent [20] in comparison with the evacuated tube collectors (ETCs), compound parabolic collectors CPCs, and flat plate collectors FPCs, which achieved 13.4%, 7.8%, and 6.5%, respectively [26-30].

According to Bava et al. [10], the annual useful energy transferred using TRNSYS software was 1.2% higher than the value obtained using an experimental study, with basis deviations of -8% for January-May and +7% for June-December. In another approach, the comparison study presented by Delgado-Torres and García-Rodríguez [31] showed that the energy performance recovered by the experimental study was less than that achieved by TRNSYS, about 3%.

This study presents the simulation of a combined STS and power cycle model. Utilization of the STEC and TESS library of the TRNSYS software [11], for Irbid city in Jordan and meteorological data supplied by the Meteonorm software.

2. METHODOLOGY

The system is composed of the solar system Concentrating solar power (CSP) and vapor power cycle (Rankin cycle). The power cycle is driven by the heat, which is produced by the solar system as shown in Figure 1. The components of the steam cycle are steam generators (Overheater, Evaporator and Economizer).

Presentation of the CSP –thermal power plant used CSP technologies-The Parabolic Trough Solar Collector (PTC) type can be used to generate electricity during the sunny day hours throughout the year. This technology has the ability to store energy as a result of its configuration, which consists of a mirror that concentrates the sun's light energy and converts it to heat. Then, heat can be used to generate steam to produce electrical energy through a steam turbine. The PTC contains a receiver tube (RT) and a parabolic-cylindrical mirror (parallel rows of long, semi-cylindricals) which circles around the RT to increase the concentration of radiation. The sun's radiation is concentrated on a longitudinal RT which is arranged along the installation. A Heat Transfer Fluid (HTF) – a type of THERMINOL VP-1 - circulates inside the RT, which is used to capture and transport the absorbed heat; the thermal liquid temperature can reach up to 300℃. The THERMINOL VP-1 used as a thermal liquid circulates inside the solar field (PTC) in order to overcome the mechanical constraints in the case of the immediate evaporation of water in the solar collector [32-34]. Moreover, the heat is transmitted to the cold water and transferred it to the steam (at efficiency in the range of 14-21%), which is used to operate the steam turbine. This system is made up of molten salt storage that can be kept during non-sunday hours.

Three stages of the steam turbine (low pressure LP, intermediate pressure IP, and high pressure HP), collector field (PTC), preheater, degasser, sub-cooler, condenser, and pump. The aim of the collector field is to generate electricity from the thermal system. The system consists of the PTC connected to the steam turbine - Rankine cycle through a set of heat exchangers. The average temperature of the thermal fluid increases according to the weather during the day and year (8760 h). The heat transfer fluid (thermal fluid) is pumped to the steam generator (economizer, evaporator, and superheater) at a constant flow rate. The HTF exchanges its heat with water (working fluid) through a heat exchanger where the HFT flows in the opposite direction of water flow. As shown in Figure 1, the HFT passes through the superheater to raise the temperature of the steam generated in the evaporator, then through the evaporator to release its heat and convert the warm water phase to a vapor. The HFT exits from the last stage of the steam generator and releases the last portion of its heat to heat the water inside the economizer, which leads to an increase in the water temperature. Then the HFT returns to the solar field to absorb the solar energy again. In the power cycle, the superheated steam completes its cycle by passing through three stages of the steam turbine.
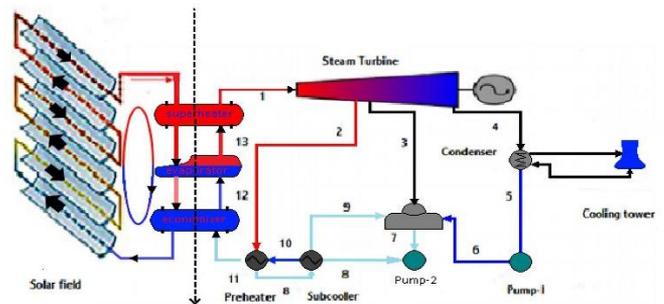
Figure 1. Schematic diagram of the thermal power cycle - solar field system

The steam turbine is divided into three stages: LP, IP, and HP, which all communicate with the preheaters (feed-water heaters). A portion of the steam (approximately 0.13% of steam) is withdrawn during the expansion and is used to heat the feed water in order to increase the efficiency of the cycle. The remaining saturation steam exits from the LP stage with low enthalpy and enters the condenser. In the condenser, the steam releases its heat and condenses. Two pumps are used to increase the pressure as required by the steam generator and the water passes through a degreaser in order to remove the melted gases before entering the steam generator.

3. TRNSYS SIMULATION SOFTWARE ASSUMPTION

Transient systems simulation is an integral, extremely flexible and extensible simulation environment used to simulate the behavior of transient systems. Transient systems simulation is an integral, extremely flexible, and extensible simulation environment used to simulate the behavior of transient systems. The TRNSYS library covers many of the elements commonly found in electrical and thermal energy systems, in addition to component systems to control the input of weather data and obtain simulation results. TRNSYS's nature provides the program with a high degree of flexibility, and it is possible to add mathematical models not included in TRNSYS's library. It advised using TRNSYS to analyze any system behavior that depends on the passing time. Recently, TRNSYS has become, for many researchers, a reference software to simulate any transient system.

The system, as depicted in Figure 2, was implemented in the TRNSYS workspace. in Figure 2, the Parabolic trough

collector (Type 398) is connected to the superheater and economizer modeled on Type 315 and to the Evaporator modeled on Type 316. The steam generator unit (superheater, economizer, and evaporator) is linked to the steam turbine (Type 318). There are two pumps: a feed pump (Type 300) and a condensate pump (Type 300) that supplies water to the sub-cooler.

Also, as illustrated in Figure 2, the HP and IP stages of the steam turbine are connected to the preheater (Type 317) and sub-cooler (Type 320). The model shown in Figure 2 consists of solar fields (PTC) of 200000 m^2. Solar zenth and azimuth angles are given by a file of the weather for Irbid city, north Jordan, which includes weather data reading and processing (TYPE109-TMY2) for a whole year. PTC has been built and tested [25]. The average exit temperature of the thermal fluid is about 280°C.

Table 1 shows the main components used in the simulations for a combined solar thermal system and power cycle in Irbid city. In addition, Table 1 contains the details of the principal parameters of the components of the model.
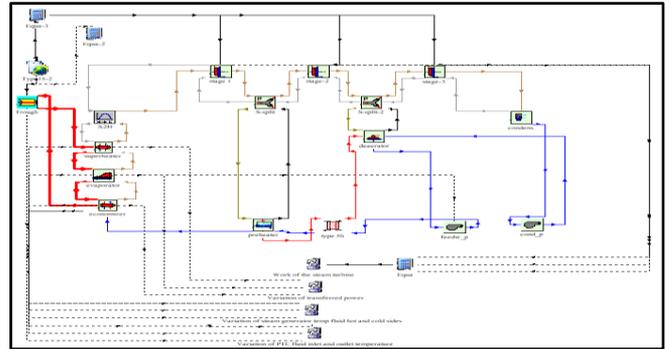
Figure 2. Model of solar thermal system combined with Rankine Cycle

Table 1. The main input specifications of the components using TRNSYS simulation software

Component	Type	Input specification	Value		
Parabolic trough collector (PTC)	TYPE396	Cw- Loss coef.	0		
		D - Loss coef.	-0.096		
		Clean Reflectivity	0.94		
		Fraction of Broken Mirror	0.0		
		SCA length, (m)	14.37		
		SCA aperture Width, (m)	1.52		
		SCA- Focal Length, (m)	0.45		
		Row spacing, (m)	4.54		
		Total Area of field, (m^2)	200000		
		Cold side flow rate, (kg/s)	12.4		
Superheater and economizer	TYPE 315	Overall heat transfer coefficient of exchanger, (KJ/hr. K)	1037068.37(SUP) 3055710.24(ECO)		
		Counter flow mode	2		
		Cold side- pressure loss "ref", (bar)	1		
		overall heat transfer factor	8164463.48		
Evaporator	TYPE 316	Pressure loss "ref", (bar)	1		
		Flow rate-Reference, (Kg/s)	12.14		
X2X	TYPE 391	Temperature -converting of water vapour into enthalpies	-		
Weather data reading and processing	TYPE109-TMY2	Irbid-. Jordan	-		
S-split		Constant gas flow in time runs.	-		
Online plotter	TYPE 389	Simulate a vapor separator to allow extraction.	-		
Turbine	TYPE 318	Stage	LP	IP	HP
		Flow rate, (kg/s)	12.14	9.92	8.82
		Inner efficiency, %	84	85	86
		design inlet pressure, (bar)	100	23.89	2.875
		design outlet pressure, (bar)	23.89	2.875	0.08
Condenser	TYPE 383	dT Cool water out condensing temp (delta C)	4		
		Temperature increase in cool. Water (delta C)	15		
Condenser pump and feed pump	TYPE 300	TYPE	CP	FP	
		Fluid specific heat, (KJ/kg.K)	4.18	4.19	
		Maximum flow rate, (kg/s)	8.525	8.525	
		Maximum power, (KW)	1	1	
Preheater	TYPE 317	Cold side fluid- specific heat, (kJ/kg)	4.24		
		Overall heat transfer factor (KJ/hr K)	186840		
		Cold sid fluid- flow rate (Kg/s)	12.14		
Subcooler	TYPE 320	Hot side fluid - Specific (KJ/Kg K)	3.355		
		Cold side fluid - Specific heat (KJ/Kg K)	4.240		

4. RESULT AND DISCUSSION

The advanced model requires the site's geographical position and the typical metrological year (TMY) data that generates hourly metrological data, which includes wind speed and ambient temperature. The Global Land Data Assimilation System (GLDAS-version 1) provides estimates for all of the variables studied. The Global Data Assimilation System is a system of operational atmospheric analysis that combines a model of the global climate–a numerical depiction of the energy fluxes and physical processes occurring in the earth's atmosphere, land surface, and oceans–with a diverse set of

satellite-derived analyses and observations. In order to run the simulation for one year and to predict the system, the TMY of Irbid is used at the GMT+2 time zone, latitude 32.5514450 N, and longitude 35.851479.

4.1 Solar radiation, dry bulb temp and wind speed

The total horizontal radiation (direct and diffuse radiation on the horizontal surface) in Irbid city is evaluated as shown in Figure 3a. During the months of May and June, the maximum radiation obtained is approximately 1145 W/m².

It is noted that Irbid city has high irradiation, especially during June, while the lowest irradiation is received during December. The reason for that is due to the location of Irbid, the scarcity of clouds, and the low humidity, which positively affects the arrival of direct horizontal solar radiation to the earth.

(a)

(b)

(c)
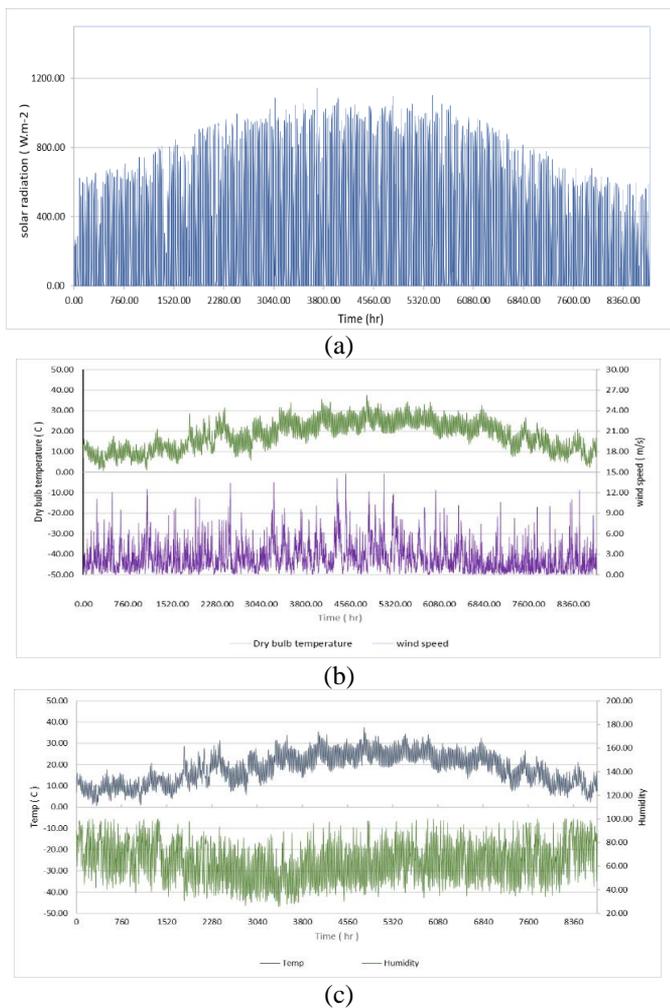
Figure 3. (a). Solar radiation in Irbid city; (b). Wind speed and dry bulb temp over year in Irbid; (c). A variations in temperature and annual average humidity in Irbid

Figure 3c shows ambient temperature over the year. The period between May and Jun is characterized by maximum ambient temperature and speed wind (see Figure 3b). Wind speed seems to have a significant impact on the energy production of a solar module. Indeed, the heat transfer coefficient may be defined as a function of total irradiance, ambient temperature, and wind speed. This coefficient particularly follows a linear law instead of the constant value

usually taken into consideration by PV software such as PVsyst.

The maximum ambient temperature and speed of wind registered were 37°C and 14.772 m/s., respectively. That is related to the total sunshine hours during the summer, which are longer than those during the winter. In addition, the sun's steadiness in the northern hemisphere, as the rays of the sun are almost perpendicular during the summer to the surface of the earth, makes the earth absorb most of the radiation energy and only a small portion is reflected from it, unlike in winter where the rays are highly inclined, which leads to reflecting the radiation without absorption.

The annual average humidity over the year. For the variation of the average annual moisture content in Irbid, it has been observed that it is lower during summer (range of 0.48-0.63) than winter (range of 0.63-0.82).

4.2 Thermal performance evaluation of the system

The curve illustrated in Figure 4a shows that at the beginning of the heating on January 1, at t=0 (24:00), the outlet temperature of the coolant is equal to the temperature of the injected fluid. After the sun rises, this temperature increases with the solar radiation concentrated on the concentrator opening. The temperature reaches 240 °C between 7:00 h (am) and 4:00 h (pm). During the same time period, the inlet temperature reaches 217°C and rises to a maximum of 290.92°C at 11:00 h (am). During the afternoon, both inlet and outlet temperatures after 5:00 h (pm) continue to decrease until they reach zero.

(a)

(b)
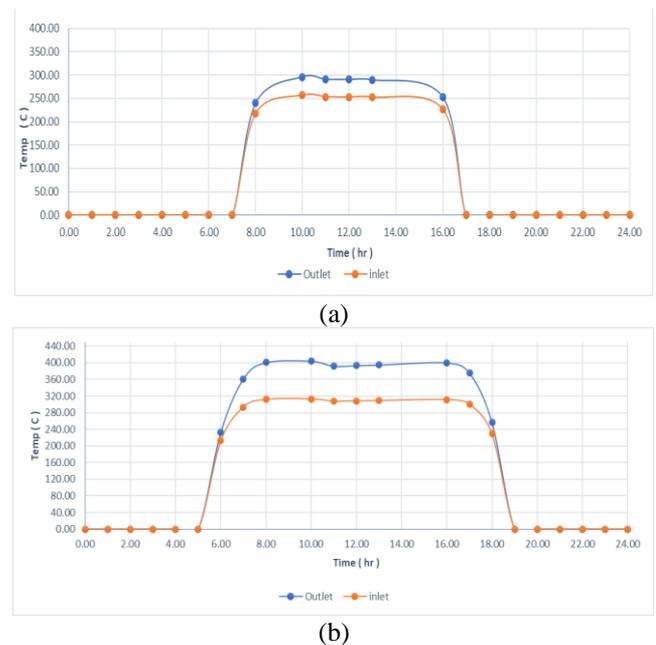
Figure 4. A Variation of PTC fluid inlet and outlet temperature (a) during the Day of January 1, (b) during the Day of August 1

Figure 4b shows the same behavior of the HTF temperature on January 1, with an increased peak temperature of the inlet and outlet of the HTF during the period of 8:00 h (am) to 4:00 h (pm). The number of sunny hours on August 1 is greater than on January 1, resulting in an increase in energy yield. Also, the irradiation is more perpendicular, which is reflected in the increment in the coolant temperature. The inlet and outlet

temperatures of the HTF reached the maximum values of 392°C and 361°C, respectively. An increment is noted before 8:00 h (am) and a decrement after 4:00 h (pm) as a result of the radiation incident angle.

4.3 Steam generator temperatures and Transferred power

The curves illustrated in Figure 5a and b show that the temperatures of the steam generator fluid on the cold and hot and cold sides increase to a peak at around 14 hr at the inlet of the steam generator. This period corresponds to maximum sun radiation. Regarding the cold side (outlet), it should be noted that the temperature will rise at each stage, reaching a maximum of 327°C at 13:00 h. After 13:00 h, the exit temperatures on each side will decrease when the sun irradiation declines until 18:00 h or they will be zero.

The temperature profiles of the steam generator fluid (working fluid) between January 1 and August 1 were obtained as shown in Figures 5a and 5b. The behavior of the temperature of the working fluid reflects the high thermal efficiency of the steam generator, with slight variance between the generator components (superheater, evaporator, and the economizer). As shown in Figure 6a and b. In this simulation, by the comparison of the inlet and outlet temperature of the coolant and working fluid, it is clearly the heat transfer between two fluids very high that will increase the system gain. This can be considered by efficiency, which can be expressed as Qout/Qin, Qout is the heat absorbed by cold water, and Qin is the heat absorbed by the working fluid.

(a)

(b)
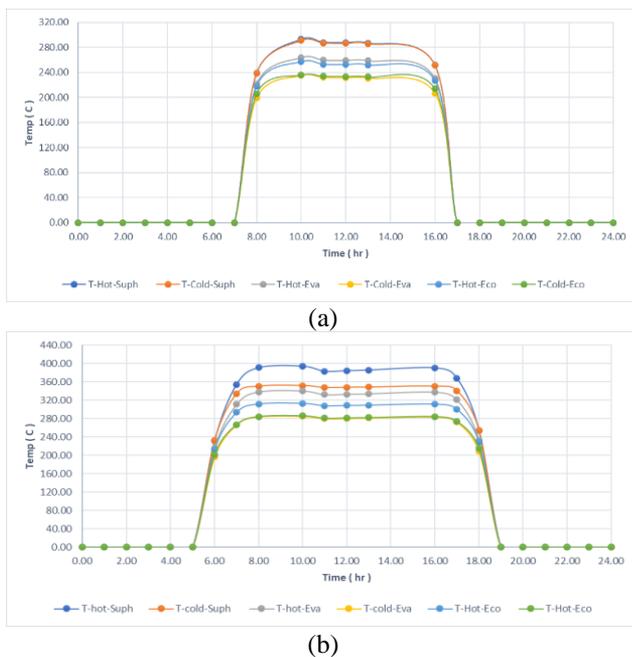
Figure 5. Variation of steam generator temperatures of the fluid on the hot and cold sides (a) during the Day of January, (b) during the Day of August 1

The curve presented in Figure 6a shows the transferred power obtained from each stage of the steam generator: superheater, evaporator, and economizer. The heat transferred to Qsup, Qeva, and Qec increases from 7:00 h (am) to a maximum value at 11:00 h (am), such that Qsup=1.99E+6 KJ/hr, Qeva=2.02E+7 KJ / hr, and Qeco=5.15E+6, then decreases to zero at 17: 00 h.

Figure 6b shows the evolution of the heat transferred on August 1 of each exchange, which indicates that the net heat transfer is higher than obtained on January 1. The heat transferred (Qsup, Qeva, and Qeco) goes into a rise from 5:00 h (am) and reaches a maximum value at 11: 00 h (am) such that Qsup=6.86E+6 KJ/hr, Qeva=3.71E+7KJ/hr and Qeco=1.76E+7, then declines in the next period to reach a zero value at 19: 00 h.

(a)

(b)
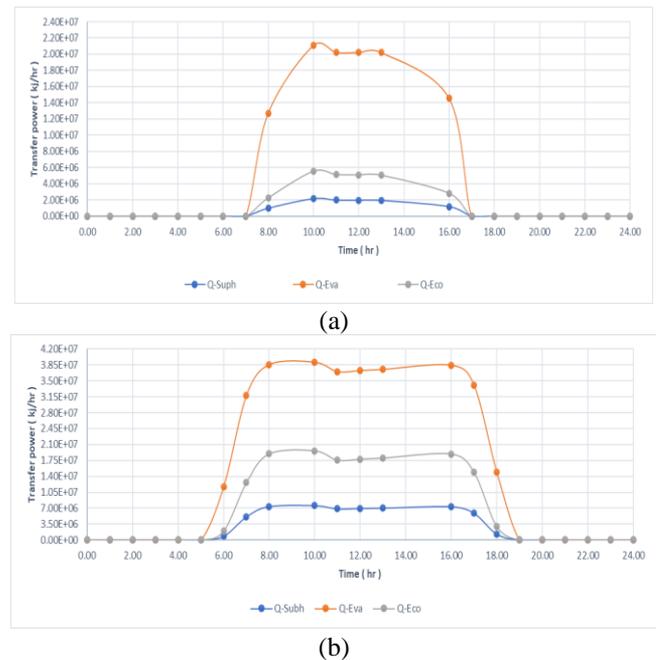
Figure 6. Transferred power variation (a) during the Day of January 1, (b) during the Day of August 1

The reason for the variation in the values between January and August is that the solar appearance period in the summer is longer than in winter, and the amount of solar radiation falling is higher in summer and this directly affects the temperatures outside of the boiler. This affects the amount of power output, which is explained by the following equation:

$$Q_{trans} = m_{hot} * cp_{hot} * (T_{hot.in} - T_{sat}) \qquad (1)$$
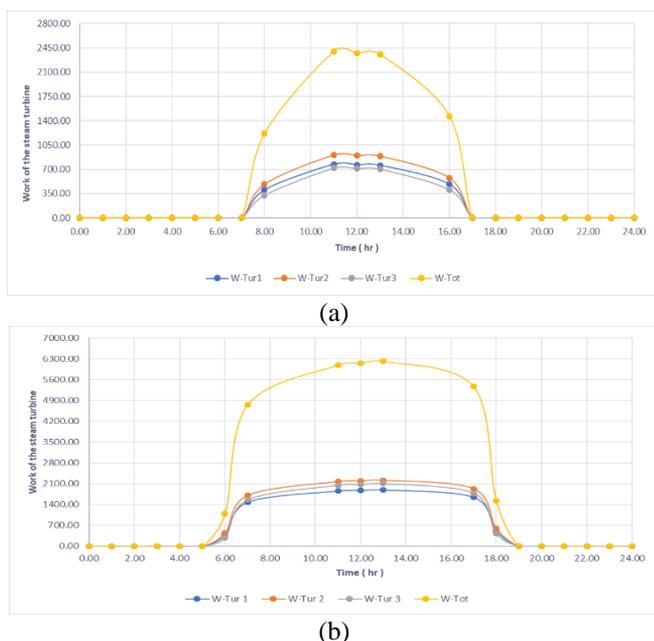
4.4 The steam turbine work

Figure 7a and b depict the variation in work obtained by the steam turbine in this simulation on January 1 and August 1. On January 1, the work begins to increase at 7:00 a.m. and continues until it reaches a maximum value of 2399 kJ/kg at 11:00 a.m., which corresponds to both heat exchange and steam-generated power. Then it decreases until it reaches zero at 17:00 h. On August 1, the work began to increase from 5:00 a.m. to a value of 6084 kJ/kg at 11:00 a.m. Then it decreases after this maximum value, so that it is zero at 19:00 h.

The reason for the variation between January and August, besides the previous reasons mentioned before, is that the steam exiting from the superheater in Augusta has a higher enthalpy than it does in January. Steam with higher enthalpy achieves more expansion and a higher power net, corresponding to the temperature difference.

$$W_{Tur} = m(h_o - h_i) \qquad (2)$$

A specific thermodynamic simulation of PTC uses TRANSYS software in order to simulate the performance during part-load conditions. In this design-model, the technical outcomes were used to back-calculate Rankine turbine efficiency and the heat exchangers.

The results showed that the PTC improves the overall solar field efficiency, the ability of PTCC to absorb both diffuse irradiance of solar and. Also, the PTC is used for high power capacity installations as its efficiency is high in the low-medium temperature ranges. This result is in close agreement with [35, 36].

(a)

(b)

Figure 7. Work (kJ/kg) variation of the steam turbine (a) during the Day of January 1, (b) during the Day of August 1

The working fluid and HTF are selected based on specific criteria: heat transfer, evaporation - temperature and temperature range [34]. The THERMINOL VP-1 and water were chosen as the best HTF and working fluid for the solar field and the three-stage Rankine cycle. results showed that the location of the site, hour number and highest solar radiation permit the positive gain of heat in the solar field and high energy production, and this is the same result obtained by most studies in the literature [32, 37, 38]. It is obvious that the temperature variations of the inlet and outlet of the PTC and heat exchanger are affected by weather variations and consequently affect the power generated from the steam turbine (LP, IP, and HP stage). It is clear that the average temperature is higher than in winter and so the generated power is higher in summer.

Moreover, the results showed that in August, compared to January, the decrease in solar radiation is 48% and the reduction in the PTC heat gain is 58%, resulting in a decrease in the power produced by the steam turbine of 67%. These results are slightly similar to the results which were obtained by Rohani et al. [39]. Furthermore, the results show that the PTC yield guarantee covers the Rankine cycle heat input, which necessitates a large area.

This simulation is applicable throughout the year and through the establishment of an integrated power plant for the production of electricity from solar energy, with the possibility of storing the excess energy with the adoption of a larger area of the solar field via solar batteries.

5. CONCLUSIONS

The integrated solar combined cycle system (ISCCS) is simulated to determine the characteristics of the system to predict the effect of varying operation conditions, such as weather and sunrise hours, on electrical power production. The ISCCS system is made up of a solar field (PTC-type) and Rankine cycle power. The ISCCS of the low temperature range-medium capacity plant was assessed. A comparison study was implemented to evaluate the efficiency, power gain and heat exchange of the proposed system for one day in January (winter) and in August (summer). The three-stage Rankine cycle was presented as a method of increasing efficiency. A portion of the steam is exported from the HP and IP stages of the turbine to preheat the feed-water. This technique decreases the energy consumed by the steam generator and consequently improves its efficiency as compared with a single stage.

This study shows ISCCS operating at temperatures as high as 400 degrees Celsius while maintaining high efficiency. The results show that the efficiency on January 1 is 14.3% and electricity power production is about 4.05 MW, while during August the efficiency achieved is 21.8% with 4.48 MW of electricity production. The results showed that the ISCRCS system's efficiency is 14.3% in winter (January 1) and 21.2% in summer (August 1), with 4.48 MW produced in winter (January 1) and 4.05 MW produced in summer (August 1).

REFERENCES

[1] Albezuirat, M.K., Hussain, M.I., Al-saraireh, F., Rosmaini, R.A. (2018). Jordan energy sector choices and challenges. SEISENSE Journal of Management, 1(5): 16-37. https://doi.org/10.5281/zenodo.1452373

[2] Blanco, J., Palenzuela, P., Alarcón-Padilla, D., Zaragoza, G., Ibarra, M. (2013). Preliminary thermoeconomic analysis of combined parabolic trough solar power and desalination plant in port Safaga (Egypt). Desalination and Water Treatment, 51(7-9): 1887-1899. https://doi.org/10.1080/19443994.2012.703388

[3] Liang, H., You, S., Zhang, H. (2015). Comparison of different heat transfer models for parabolic trough solar collectors. Applied Energy, 148: 105-114. https://doi.org/10.1016/j.apenergy.2015.03.059

[4] Kicsiny, R. (2014). Multiple linear regression based models for solar collectors. Solar Energy, 110: 496-506. https://doi.org/10.1016/j.solener.2014.10.003

[5] Farjana, S.H., Huda, N., Mahmud, M.A.P., Saidur, R. (2018). Solar process heat in industrial systems—A global review. Renewable and Sustainable Energy Reviews, 82: 2270-2286. https://doi.org/10.1016/j.rser.2017.08.065

[6] Shrivastava, R.L., Kumar, V., Untawale, S.P. (2017). Modeling and simulation of solar water heater: A TRNSYS perspective. Renewable and Sustainable Energy Reviews, 67: 126-143. https://doi.org/10.1016/j.rser.2016.09.005

[7] Sornek, K. (2016). The comparison of solar water heating system operation parameters calculated using traditional method and dynamic simulations. In E3S Web of Conferences; EDP Sciences: Les Ulis, France, 10: 4. https://doi.org/10.1051/e3sconf/20161000137

[8] Al bkoor Alrawashdeh, K., Al-Zboon, K.K., Momani, R.,

Momani, T., Gul, E., Bartocci, P., Fantozzi, F. (2022). Performance of dual multistage flashing-recycled brine and solar power plant, in the framework of the WATER-ENERGY nexus. Energy Nexus, 100046. https://doi.org/10.1016/j.nexus.2022.100046

[9] Xu, L., Wang, Z.F., Yuan, G.F., Sun, F.H., Zhang, X.L. (2015). Thermal performance of parabolic trough solar collectors under the condition of dramatically varying DNI. Energy Procedia, 69: 218-225. https://doi.org/10.1016/j.egypro.2015.03.025

[10] Bava, F., Dragsted, J., Furbo, S. (2017). A numerical model to evaluate the flow distribution in a large solar collector field. Solar Energy, 143: 31-42. https://doi.org/10.1016/j.solener.2016.12.029

[11] Farjana, S.H., Huda, N., Mahmud, M.A.P., Saidur, R. (2018). Solar process heat in industrial systems-A global review. Renewable and Sustainable Energy Reviews, 82: 2270–2286. https://doi.org/10.1016/j.rser.2017.08.065

[12] Xu, L., Wang, Z.F., Yuan, G.F., Sun, F.H., Zhang, X.L. (2015). Thermal performance of parabolic troughsolar collectors under the condition of dramatically varying DNI. Energy Procedia, 69: 218-222. https://doi.org/10.1016/j.egypro.2015.03.025

[13] Shrivastava, R.L., Kumar, V., Untawale, S.P. (2017). Modeling and simulation of solar water heater: A TRNSYS perpective. Renewable and Sustainable Energy Reviews, 67: 126-143. https://doi.org/10.1016/j.rser.2016.09.005

[14] Frey, P., Fischer, S., Drück, H., Jakob, K. (2015). Monitoring results of a solar process heat system installed at a textile company in Southern Germany. Energy Procedia, 70: 615-620. https://doi.org/10.1016/j.egypro.2015.02.168

[15] Wojcicki, D.J. (2015). The application of the typical day concept in flat plate solar collector models. Renewable and Sustainable Energy Reviews, 49: 968-974. https://doi.org/10.1016/j.rser.2015.04.128

[16] Situmbeko, S.M., Inambao, F.L. (2015). Heat exchanger modelling for solar Organic Rankine Cycle. International Journal of Thermal & Environmental Engineering, 9(1): 7-16. http://dx.doi.org/10.5383/ijtee.09.01.002

[17] Kizilkan, Ö., Nižetić, S., Yildirim, G. (2016). Solar assisted organic rankine cycle for power generation: A comparative analysis for natural working fluids. In Energy, Transportation and Global Warming, pp. 175-192. http://dx.doi.org/10.1007/978-3-319-30127-3

[18] Lauterbach, C., Schmitt, B., Jordan, U., Vajen, K. (2012). The potential of solar heat for industrial processes in Germany. Renewable and Sustainable Energy Reviews, 16: 5121-5130. http://dx.doi.org/10.1016/j.rser.2012.04.032

[19] Pietruschka, D., Fedrizzi, R., Orioli, F., Söll, R., Stauss, R. (2012). Demonstration of three large scale solar process heat applications with different solar thermal collector technologies. Energy Procedia, 30: 755-764. https://doi.org/10.1016/j.egypro.2012.11.086

[20] Mauthner, F., Hubmann, M., Brunner, C., Fink, C. (2014). Manufacture of malt and beer with low temperature solar process heat. Energy Procedia, 48: 1188-1193. https://doi.org/10.1016/j.egypro.2014.02.134

[21] Muster, B., Ben Hassine, I., Helmke, A., Heß, S., Krummenacher, P., Muster, B., Schmitt, B., Schnitzer, H. (2015). Solar Process Heat for Production and Advanced Applications: Integration Guideline; IEA SHC Task 49HC Task 49—Deliverable B2; Solar Heating and Cooling Programe: Paris, France, 2015. https://www.academia.edu/28599671/A_Solar_Process_Heat_for_Production_and_Advanced_Applications_integration_guideline_final_2015.

[22] Schramm, S., Adam, M. (2014). Storage in solar process heat applications. Energy Procedia, 48: 1202-1209. https://doi.org/10.1016/j.egypro.2014.02.136

[23] Lauterbach, C., Schmitt, B., Vajen, K. (2014). System analysis of a low-temperature solar process heat system. Solar Energy, 101: 117-130. https://doi.org/10.1016/j.solener.2013.12.014

[24] Okoroigwe, E., Madhlopa, A. (2016). An integrated combined cycle system driven by a solar tower: A review. Renewable and Sustainable Energy Reviews, 57: 337-350. http://dx.doi.org/ 10.1016/j.rser.2015.12.092

[25] Tian, Y., Zhao, C.Y. (2013). A review of solar collectors and thermal energy storage in solar thermal applications. Applied Energy, 104: 538-553. http://dx.doi.org/10.1016/j.apenergy.2012.11.051

[26] Behar, O., Khellaf, A., Mohammedi, K., Ait-Kaci, S. (2014). A review of integrated solar combined cycle system (ISCCS) with a parabolic trough technology. Renewable and Sustainable Energy Reviews, 39: 223-250. http://dx.doi.org/10.1016/j.rser.2014.07.066

[27] Manolakos, D. (2006). Development of an Autonomous Low-Temperature Solar Rankine Cycle System for Reverse Osmosis Desalination.

[28] Manolakos, D., Papadakis, G., Essam, S.M., Kyritsis, S., Bouzianas, K. (2005). Design of an autonomous low-temperature solar Rankine cycle system for reverse osmosis desalination. Desalination, 183: 73-80. http://dx.doi.org/10.1016/j.desal.2006. 04.018

[29] Manolakos, D., Papadakis, G., Kyritsis, S., Bouzianas, K. (2007). Experimental evaluation of an autonomous low-temperature solar Rankine cycle system for reverse osmosis desalination. Desalinatio, 203: 366-374. http://dx.doi.org/10.1016/j.desal. 2006.04.018

[30] Delgado-Torres, A.M., García-Rodríguez, L. (2010). Analysis and optimization of the low temperature solar organic Rankine cycle (ORC). Energy conversion and Management, 51: 2846-2856. http://dx.doi.org/10.1016/j.enconman.2010.06.022

[31] Delgado-Torres, A.M., García-Rodríguez, L. (2010). Preliminary design of seawater and brackish water reverse osmosis desalination systems driven by low-temperature solar organic Rankine cycles (ORC). Energy Conversion and Management, 51(12): 2913-2920. http://dx.doi.org/10.1016/j.enconman.2010.06.032

[32] Almeida, P., Carvalho, M.J., Amorim, R., Mendes, J.F., Lopes, V. (2014). Dynamic testing of systems—Use of TRNSYS as an approach for parameter identification. Solar Energy, 104: 60-70. https://doi.org/10.1016/j.solener.2014.02.010

[33] Pitz-Paal, R., Jones, S.A. (1998). A TRNSYS Model Library for Solar Thermal Electric Components (STEC). A Reference Manual, Release 1.0, IEA-Solar Power and Chemical Energy Systems, Task III: Solar Technologies and Applications.

[34] Al-Odat. M., Rawashedsh. K., Al-Hasan. M. (2021). Performance investigation of flat plate and evacuated tube collectors under Jordan climate conditions using TRNSYS software. Mathematical Modelling of

Engineering Problems, 8(1): 142-148. https://doi.org/10.18280/mmep.080118

[35] Desai, N.B., Bandyopadhyay, S. (2015). Optimization of concentrating solar thermal power plant based on parabolic trough collector. Journal of Cleaner Production, 89: 262-271. http://dx.doi.org/10.1016/j.jclepro.2014.10.097

[36] Dayem, A.M.A., Metwallya, M.M., Alghamdi A.S., Marzoukb, E.M. (2014). Numerical simulation and experimental validation of integrated solar combined power plant. Energy Procedia, 50: 290-230. http://dx.doi.org/10.1016/j.egypro.2014.06.036

[37] Uçkun. C. (2013). Modeling and simulations of direct steam generation in concentrating solar power plants using parabolic trough collectors. Thesis. The Graduate School of Natural and Applied Science. Middle East Technical University. https://hdl.handle.net/11511/22381

[38] Chaanaoui, M., Vaudreuil, S., Bounahmidi, T. (2016). Benchmark of concentrating solar power plants: historical, current and future technical and economic development. Procedia Computer Science, 83: 782-789. https://doi.org/10.1016/j.procs.2016.04.167

[39] Rohani, S., Fluri, T.P., Dinter, F., Nitz, P., (2017). Modelling and simulation of parabolic trough plants based on real operating data. Solar Energy, 158: 845-860. https://doi.org/10.1016/j.solener.2017.10.023